20th International Conference on Composite Materials
Copenhagen, 19-24th July 2015

MODELLING OPEN CELL FOAMS BASED ON 3D IMAGE DATA

A. Liebscher[1], H. Andrä[2], M. Kabel[2], D. Merkert[1] and C. Redenbach[1]

[1]Department of Mathematics, University of Kaiserslautern
P.O. Box 3049, D-67653 Kaiserslautern, Germany
Web page: www.mathematik.uni-kl.de
Email: liebscher@mathematik.uni-kl.de, dmerkert@mathematik.uni-kl.de,
redenbach@mathematik.uni-kl.de

[2]Department of Flow and Material Simulation, Fraunhofer ITWM
Fraunhofer-Platz 1, D-67663 Kaiserslautern, Germany
Web page: www.itwm.fraunhofer.de
Email: heiko.andrae@itwm.fraunhofer.de, matthias.kabel@itwm.fraunhofer.de

Keywords: Laguerre tessellation, microstructure model, elastic moduli, micro-computed tomography

ABSTRACT

The macroscopic properties of open cell foams are highly influenced by the foam's microstructure. Recent research has shown that the complex functional behaviour of foams can be studied by an exact characterisation of their microstructure followed by numeric simulations. The key element of such studies is the microstructure model of the foam. Models from stochastic geometry in conjunction with X-ray computed tomography have turned out to be powerful tools in this context.

We focus on the realistic reproduction of the foam's microstructure in a model. Using various geometric characteristics of the cell and strut system, we propose a two step model fitting procedure: First, a Laguerre tessellation model is fitted to the cell system of the foam. In the second step, we estimate the local thickness of the foam's edge system and fit a polynomial model to describe the locally varying thickness distribution. The edge system of the tessellation is then adaptively dilated using the polynomial model as size map to form the struts of the foam.

The elastic properties of the resulting microstructure model are evaluated using an iterative FFT-based algorithm. By comparing the effective material properties of the real foam and its model, we found the response of the model in very good agreement with the real foam. These findings support the supposition that exact microstructure models play a vital role in the study of the functional behaviour of foams.

1 INTRODUCTION

In the recent years, the combination of quantitative image analysis, stochastic microstructure modelling and numerical prediction of macroscopic properties has been established as powerful means to gain an understanding of the complex relations between a material's microstructure geometry and its macroscopic behaviour. Once a model has been fit to the observed microstructure, variation of the model parameters allows for the generation of new model realisations with modified microstructure characteristics. This opens the road to a virtual design of materials for particular fields of application. In the present paper, we will demonstrate these techniques on the example of an open cell foam.

The main step in this procedure consists in fitting a random tessellation to the cell system of the foam. One of the most well-known tessellation models is the Voronoi tessellation. It is generated by a locally finite set $\varphi = \{x_1, x_2, \ldots\} \subseteq \mathbf{R}^d$ by assigning to each point $x \in \varphi$ the set $C(x)$ of those points in space having x as nearest neighbour in φ. However, the Voronoi construction with cell facets being equidistant from the generators of their cells is quite restrictive for the range of cell patterns which can be realised by Voronoi tessellations. More flexible models are obtained by weighted generalisations.

Property		Sample	Model	
			Mean	Dev. [%]
V [mm^3]	Mean	54.12	54.07	−0.10
	SD	9.97	10.24	+2.66
S [mm^2]	Mean	85.01	76.88	−9.56
	SD	10.32	8.98	−12.00
$\bar{b}$ [mm]	Mean	5.26	5.15	−2.12
	SD	0.30	0.40	+33.75
n_{32}	Mean	13.92	14.24	+2.32
	SD	1.45	1.54	+5.58

Table 1: Deviation between geometric characteristics of the cell model and the scaled foam cells.

Laguerre tessellations are particularly suitable for modelling the cell systems of foams. The points of φ are assigned positive weights such that each pair $(x, r) \in \varphi$ can be interpreted as a sphere with centre x and radius r. Then the *Laguerre cell* of $(x, r) \in \varphi$ is defined as

$$C\big((x,r),\varphi\big) = \{y \in \mathbf{R}^d : ||y-x||^2 - r^2 \leq ||y-x'||^2 - r'^2,\ (x',r') \in \varphi\}\,. \tag{1}$$

If all radii are equal, the special case of the Voronoi tessellation is obtained.

In the following we study an open cell copper foam of dimensions 250 mm × 25 mm × 25 mm. Its microstructure is analysed using micro computed tomography (µCT), for which we cut a cube with an edge length of 25 mm from the rod, resulting in an image of 630 × 630 × 630 voxels with an isotropic edge length of 38.15 µm. The presented results revise and extend the work done in [1, 2], see also [3, Chap. 7].

2 MODELLING THE CELL SYSTEM

To fit a model to the cell system of the foam, empirical distributions of cell size and shape are necessary. These characteristics are estimated from the µCT image of a foam using the cell reconstruction procedure described in [4]. If parametrised properly [3, Sec. 3.3], this procedure divides the pore space of the foam into cells whose edges coincide with the foam's strut system. For the modelling we then interpret the reconstructed cell system of the foam as a realisation of a stationary and isotropic random tessellation, that is, a random tessellation whose distribution is motion invariant.

In practice, however, real foams are often anisotropic along the rise direction. To deal with this anisotropy, the cell system of the foam is rescaled such that the mean Feret diameters of the cells along the three coordinate axes are equal. Subsequently, an isotropic model is fitted to the scaled cell system. Reverting the scaling then yields a model for the observed cell system of the foam.

The cells of real foams show a high degree of regularity. A model that is able to reproduce this regularity is a Laguerre tessellation generated by a dense random system of nonoverlapping balls. Besides their innate regularity these models have the advantage that each Laguerre cell completely contains its generating ball. Consequently, the volume distribution of the cells in the model is controlled, to a certain degree, by the volume distribution of the balls (see e. g. [5, Fig. 3]).

The deviation of the model from the real foam is defined by the relative Euclidean distance [6], i. e.

$$d(c,\hat{c}) = \sqrt{\sum_{i=1}^{n}\Big(\frac{\hat{c}_i - c_i}{\hat{c}_i}\Big)^2}\,, \tag{2}$$

where the entries of $\hat{c} = (\hat{c}_1, \ldots, \hat{c}_n)$ and $c = (c_1, \ldots, c_n)$ denote suitable geometric characteristics of the cells of the observed foam and the model, respectively. These characteristics are estimated from the µCT

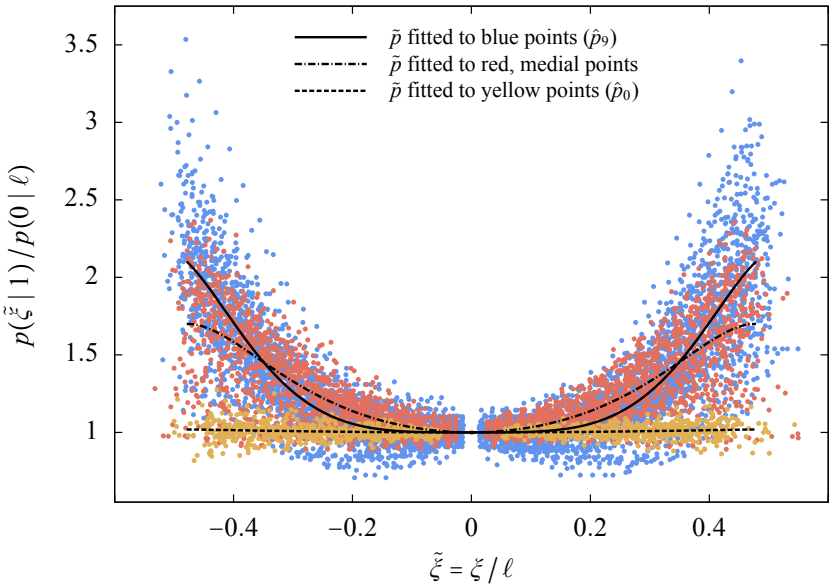

Figure 1: Plot of the thickness profile for the shortest (foreground points, yellow), medial (intermediate points, red), and longest (background points, blue) 10 % of the struts normalised by $p(0 \mid \ell)$ and ℓ. Polynomials were fitted using weighted least squares.

image of a foam after reconstructing the foam cells as mentioned above. In our study we use the means and standard deviations of the cell volume V, the surface area S, the number of faces n_{32}, and the mean breadth $\bar{b}$ [7].

If a parametric model, i.e. an algorithm for generating the ball packing and a parametric distribution for the volume distribution of the balls, is fixed, there will typically be two free parameters: the packing fraction τ and the coefficient of variation c of the volume distribution. These parameters can be estimated by minimising Equation (2) using a Monte Carlo simulation. An alternative approach was presented in [5], where Laguerre tessellations of dense ball packings with lognormally and gamma distributed volumes were generated for various packing fractions τ and coefficients of variation c. Subsequently, polynomials in c were fitted to the estimated geometric characteristics for each value of τ. With these results the minimisation of Equation (2) reduces to the minimisation of a polynomial.

For our sample the best fit was obtained for lognormally distributed ball volumes with parameters $\tau = 0.6$ and $c = 0.223$. A comparison of the characteristics of the observed cell system and the average over five realisations of the model is shown in Table 1. The model is in good agreement with the real structure. With exception of the mean surface area and the standard deviations of the surface area, the mean breadth and the number of faces, the geometric characteristics of the model differ by at most 3 %.

The deviation of about 33 % of the standard deviation of the mean cell diameter is caused by comparing the results from two different estimation techniques: In the image the mean breadth is estimated by evaluating 13 directions [8, Sec. 5.2] whereas in the model the exact formula for convex polytopes is applied [9, p. 244]. [5, 10] report similar errors of above 20 %. However, the next sections show that this deviation has no negative influence on the geometric and physical properties of the derived microstructure model.

The approximately 6 % higher standard deviation of the number of faces per cell in the model is caused by small triangular faces. These are common in Laguerre tessellations generated from ball packings but absent in real foams owing to the surface energy minimisation during the formation process of the foam. Another consequence of the energy minimisation is the difference between the moments of the surface area distribution in the model and the foam. It is caused by the approximation of curved foam cells by flat polyhedra [11].

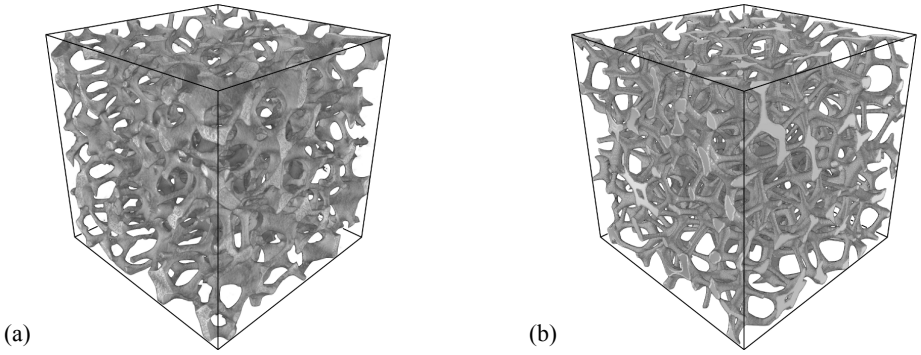

(a) (b)

Figure 2: Visualisation of the real foam (a) along with a realisation of the microstructure model (b). Shown is a volume of 430^3 voxels.

3 MODELLING THE STRUT SYSTEM

The microstructure of an open foam is defined by an interconnected network of struts. It is modelled by morphologically dilating the edge system of the tessellation model by a ball. A typical feature of the struts in real foams is their locally varying thickness, that is, struts are thicker at the nodes than in the centre. To include the varying strut thickness in the model, we use the concept of locally adaptive morphology introduced in [12]. This concept allows location adaptive ball sizes which are computed as follows.

We denote the mean thickness of struts with length ℓ at distance $\xi \in [-\ell/2, \ell/2]$ from their centre by $p(\xi \mid \ell)$. As a measure for the strut thickness, we use the radius of the maximal inscribed ball. By normalising $p(\xi \mid \ell)$ by the mid-span thickness $p(0 \mid \ell)$ and the strut length ℓ, we get a scale free representation of the strut thickness.

To estimate the local strut thickness from the µCT image of the foam, the skeleton of the foam is computed as introduced in [13]. By skeleton we understand the smallest (but not necessary unique) medial subset of the binarised foam image with the same shape as the foam. The resulting spherical contact profiles for the shortest, medial, and longest 10 % of the copper foam's struts normalised by $p(0 \mid \ell)$ and ℓ are shown in Figure 1. The differences between the three deciles disprove the assumption made in [14] that the strut thickness scales with length. More details can be found in the discussion of [3, Chap. 6] or in [13, 15].

The size map for the strut thickness model is obtained by fitting a polynomial to certain length classes of the normalised spherical contact profile. We found that the best performing polynomial model in [13] is also the optimal choice for the observed copper foam. It is defined by

$$\tilde{p}(\tilde{\xi}) = p_0(a\tilde{\xi}^2 + b\tilde{\xi}^4 + c\tilde{\xi}^8 + 1) \qquad \text{with} \qquad a, b, c \in \mathbf{R}\,, \tag{3}$$

where $\tilde{\xi} = \xi/\ell$ denotes the distance from the strut centre ξ normalised by the strut's length ℓ. The mid-span thickness p_0 in the model is chosen to be a free parameter to adjust the characteristics of the individual struts.

To fit a polynomial model to the observed profiles, we subdivide the data into ten length decile classes $q_i = (x_i, x_{i+1}]$ with $i = 0, \ldots, 9$, where x_i denotes the ith decile of the strut length distribution. We set $p_0 = 1$ and then use weighted least squares to individually determine the coefficients a_i, b_i, and c_i of the model in

$$\hat{p}_i(\tilde{\xi}) = a_i\tilde{\xi}^2 + b_i\tilde{\xi}^4 + c_i\tilde{\xi}^8 + 1 \tag{4}$$

for all normalised values of $p(\tilde{\xi} \mid \ell)$ with $\ell \in q_i$. The coefficients of the polynomials $\hat{p}_i$ of the copper foam for the different deciles can be found in [3, Tab. 7.2]. A plot of $\hat{p}_0$ and $\hat{p}_9$ is shown in Figure 1.

The size map for the adaptive dilation of the edge system is defined by the edge length classes given by q_i. To get a smooth transition between two adjacent struts, the maximal value of each $\hat{p}_i$ (the thickness

		Model	
Property	Sample	Mean	Dev. [%]
V_V	0.1203	0.1228	+2.09
S_V [mm^{-1}]	6.7485×10^5	6.5323×10^5	−3.20
M_V [mm^{-2}]	8.3066×10^{11}	7.4876×10^{11}	−9.86
χ_V [mm^{-3}]	-1.4954×10^{17}	-1.4787×10^{17}	−1.12

Table 2: Comparison of the densities of the intrinsic volumes of the copper foam and the average over five realisations of its microstructure model. The coefficient of variation between the realisations of the model is for all properties smaller than $1/150$.

in the nodes) was fixed to the median node radius $r_N = 0.55\,\mathrm{mm}$. This is achieved by setting the mid-span thickness to $p_0 = r_N/\hat{p}_i(0.5)$ for all i. Visualisations of the real foam and one realisation of its model are shown in Figure 2.

Recall the stochastic nature of the microstructure model. From a deterministic point of view, it may differ significantly from the real foam as indicated in Figure 2. Hence, both must be compared in a stochastic sense, that is, the model has to resemble the distribution of certain geometric characteristics of the real foam. Therefore, we validated the model by comparing estimates of its intrinsic volume densities [16] (averaged over five realisations) with the values obtained from the real foam (see Table 2 for details).

Both structures barely differ in their densities of the volume V_V (volume fraction), the surface area S_V (specific surface area), and the Euler number χ_V. The deviation of about 10 % for the density of the integral of mean curvature M_V indicates that the microstructure model has a smoother surface than the real foam. Since the roughness of the surface has an impact on the estimation of M_V this deviation is not surprising. Note that these geometric properties were reproduced automatically in the model without considering them as parameters during the model fit. That means we only provided the polynomials to describe the strut thickness and the node thickness for the generation of the microstructure model.

4 EVALUATION OF THE MECHANICAL PROPERTIES

To evaluate the mechanical properties of the microstructure model, we compute the macroscopic elastic properties of its realisations and compare the results with the ones of the real foam. For this purpose we solve the equation of static linear elasticity

$$\nabla \cdot C^0 \varepsilon = -\nabla \cdot \left(C - C^0\right)\varepsilon \tag{5}$$

in the weak sense for a given stiffness distribution tensor of fourth-order $C(x)$ on the torus $\mathbf{R}^3/\mathbf{Z}^3$. The strain field is denoted by $\varepsilon = \varepsilon_0 + 0.5\left(\nabla u + (\nabla u)^T\right)$, where $u \in H^1\left(\mathbf{R}^3/\mathbf{Z}^3\right)^3$ is the displacement field, C^0 is a constant isotropic reference stiffness, and ε_0 is the second-order tensor of the macroscopic strain applied to the microstructure geometry. In our study we used an isotropic stiffness distribution with Young's moduli $E = 100$ for the copper foam and $E = 1$ for the matrix material (air). For both materials, ν, Poisson's ratio, is set to 0.2.

With this setup, we may compute the macroscopic stiffness C^* by

$$C^* \varepsilon_0 = \int_{\mathbf{R}^3/\mathbf{Z}^3} C\varepsilon \,\mathrm{d}x\,. \tag{6}$$

If we reformulate Equation (5) into a fixed-point equation with respect to the strain, we get the Lippmann–Schwinger equation [17, 18]

$$\varepsilon = E - \Gamma^0 * \left(C - C^0\right)\varepsilon\,, \tag{7}$$

where $*$ denotes the convolution operator. Γ^0 is the solution operator derived from the fundamental operator of Equation (5).

		Model	
Modulus	Sample	Mean	Dev. [%]
E_1 [GPa]	7.29	7.15	−1.96
E_2 [GPa]	7.21	7.64	+6.01
E_3 [GPa]	7.23	7.25	+0.23
G_{12} [GPa]	3.03	3.08	+1.47
G_{13} [GPa]	3.03	3.00	−1.03
G_{23} [GPa]	3.02	3.10	+2.65
ν_{12}	0.20	0.19	−3.64
ν_{13}	0.20	0.20	+0.26
ν_{23}	0.19	0.20	+5.17

Table 3: Effective moduli of the copper foam in comparison to its microstructure model. The results for the model are averaged over five realisations.

To solve Equation (7) we apply the basic scheme of [19] directly to the digitised microstructure model with a size of 656^3 voxels. The scheme is based on a collocation with trigonometric polynomials and an efficient evaluation of the convolution with Γ^0 in Fourier space by means of the Fast Fourier transform. The computation is further accelerated by means of the conjugate gradient method proposed in [20]. The computations for this publication were done with the software package FeelMath [21].

Table 3 summarises some of the macroscopic material moduli of the copper foam in comparison with the ones that were averaged over five realisations of the model. Shown are the properties for an orthotropic macroscopic behaviour, that is, Young's moduli E_i, the shear moduli G_{ij}, and Poisson's ratios ν_{ij}. Despite its structural anisotropy, the foam sample exhibits an isotropic elastic response. The moduli of the model differ by at most 6 % whereas the coefficient of variation among the realisations of the model is smaller than $1/500$.

5 CONCLUSIONS

In this paper we presented a microstructure model of an open cell copper foam. The model is based on the adaptively dilated edge system of a Laguerre tessellation generated from a ball packing. The intrinsic volumes (with exception of the density of the mean curvature) of the microstructure model that we obtain by this procedure differ by at most 3.2 % from the values of the real foam—without separately considering them as parameters for the model fit. Also the mechanical response of the microstructure model is in good agreement with the real foam.

REFERENCES

[1] A. Liebscher and C. Redenbach. Modelling the local strut thickness of open foams based on 3d image data. *Proceedings of the International Conference on Cellular Materials, Dresden, Germany, November 7–9, 2012*.

[2] A. Liebscher and C. Redenbach. 3d image analysis and stochastic modelling of open foams. *International Journal of Materials Research*, **103**, 2012, pp. 155–161. (doi: 10.3139/146.110667).

[3] A. Liebscher. *Stochastic Modelling of Foams*. PhD thesis, Fachbereich Mathematik, TU Kaiserslautern, 2014.

[4] V. Cenens, R. Huis, B. Chauvaux, J. M. Dereppe, C. Gratin, and F. Meyer. 3d cellular structure characterization of flexible polyurethane foam. *Cellular and microcellular materials (Eds. V. Kumar, K. A. Seeler)*, Vol. 53, ASME, 1994, pp. 29–44.

[5] C. Redenbach. Microstructure models for cellular materials. *Computational Materials Science*, **44**, 2009, pp. 1397–1407. (doi: 10.1016/j.commatsci.2008.09.018).

[6] C. Gloaguen, F. Fleischer, H. Schmidt, and V. Schmidt. Fitting of stochastic telecommunication network models via distance measures and Monte-Carlo tests. *Telecommunication Systems*, **31**, 2006, pp. 353–377. (doi: 10.1007/s11235-006-6723-3).

[7] C. Lautensack. Fitting three-dimensional Laguerre tessellations to foam structures. *Journal of Applied Statistics*, **35**, 2008 , pp. 985–995. (doi: 10.1080/02664760802188112).

[8] J. Ohser and K. Schladitz. *3D Images of Materials Structures: Processing and Analysis*. Wiley-VCH, Weinheim, 2009.

[9] L. A. Santaló. *Integral Geometry and Geometric Probability*. Cambridge University Press, Cambridge, 2004.

[10] C. Lautensack, M. Giertzsch, M. Godehardt, and K. Schladitz. Modelling a ceramic foam using locally adaptable morphology. *Journal of Microscopy*, **230**, 2008, pp. 396–404. (doi: 10.1111/j.1365-2818.2008.01998.x).

[11] S. Hilgenfeldt, A. M. Kraynik, D. A. Reinelt, and J. M. Sullivan. The structure of foam cells: Isotropic plateau polyhedra. *Europhysics Letters*, **67**, 2004, pp. 484–490. (doi: 10.1209/epl/i2003-10295-7).

[12] O. Cuisenaire. Locally adaptable mathematical morphology using distance transformations. *Pattern Recognition*, **39**, 2006, pp. 405–416. (doi: 10.1016/j.patcog.2005.07.009).

[13] A. Liebscher and C. Redenbach. Statistical analysis of the local strut thickness of open cell foams. *Image Analysis & Stereology*, **32**, 2013, pp. 101–112. (doi: 10.5566/ias.v32.p1-12).

[14] W.-Y. Jang, A.M. Kraynik, and S. Kyriakides. On the microstructure of open-cell foams and its effect on elastic properties. *International Journal of Solids and Structures*, **45**, 2008, pp. 1845–1875. (doi: 10.1016/j.ijsolstr.2007.10.008).

[15] S. Gaitanaros, S. Kyriakides, and A. M. Kraynik. On the crushing response of random open-cell foams. *International Journal of Solids and Structures*, **49**, 2012, pp. 2733–2743.

[16] R. Schneider and W. Weil. *Stochastic and Integral Geometry*. Springer, Berlin, 2008.

[17] E. Kröner. *Statistical Continuum Mechanics*. Springer, Wien, 1971.

[18] R. Zeller and P.H. Dederichs. Elastic constants of polycrystals. *Physica status solidi*, **55**, 1973, pp. 831–842.

[19] H. Moulinec and P. Suquet. A fast numerical method for computing the linear and nonlinear mechanical properties of composites. *Comptes rendus de l'Académie des sciences*, **318**, 1994, pp. 1417–1423.

[20] J. Vondřejc, J. Zeman, and I. Marek. An FFT-based Galerkin method for homogenization of periodic media. *Computers & Mathematics with Applications*, **68**, 2014, pp. 156–173. (doi: 10.1016/j.camwa.2014.05.014).

[21] Fraunhofer ITWM: FeelMath. www.itwm.fraunhofer.de/feelmath. Accessed: 2015-04-15.